Capacity Limits of Information Transport in Fiber-Optic Networks

René-Jean Essiambre,* Gerard J. Foschini, Gerhard Kramer, and Peter J. Winzer

Bell Labs, Alcatel-Lucent, 791 Holmdel-Keyport Road, Holmdel, New Jersey, 07733 USA

(Received 11 April 2008; revised manuscript received 17 July 2008; published 13 October 2008)

The instantaneous optical Kerr effect in optical fibers is a nonlinear phenomenon that can impose limits on the ability of fiber-optic communication systems to transport information. We present here a conservative estimate of the ''fiber channel'' capacity in an optically routed network. We show that the fiber capacity per unit bandwidth for a given distance significantly exceeds current record experimental demonstrations.

DOI: 10.1103/PhysRevLett.101.163901 PACS numbers: 42.79.Sz, 42.81.−i, 87.19.lo, 89.70.Kn

The seminal work of Shannon published in 1948 [1] gave birth to information theory. Shannon determined the capacity of memoryless channels, including channels impaired by additive white Gaussian noise (AWGN) for a given signal-to-noise ratio (SNR). The extension of Shannon's theory to the ''fiber channel'' in optical core networks faces several major difficulties. An important challenge originates from the presence of three fundamental physical phenomena in optical fibers: noise, fiber chromatic dispersion, and the instantaneous Kerr nonlinearity. In addition, in optically routed networks, optical filters distributed in the networks route individual wavelength-division multiplexed (WDM) channels to their intended destination.

A few studies have considered the impact of the Kerr nonlinearity on fiber capacity. These studies rely on empirical approaches [2], approximate solutions assuming that fiber nonlinearity is either low [3–9] or is considered as multiplicative noise [3,4,6], are limited to specific nonlinear propagation effects [10], confined to specific binary formats [11] or do not make use of maximally compact modulation [12]. Finally, these approaches do not explicitly account for the impact of spectral confinement in optically routed networks.

In this Letter, we address fundamental capacity limits of the fiber channel in optically routed networks using a full field representation and a series of advanced techniques. We signal at near Nyquist rate [13] for maximum spectral efficiency, use multilevel modulation, and reverse nonlinear propagation at both the transmitter and receiver, the latter employing coherent detection. All elementary (instantaneous) Kerr nonlinear interactions in the presence of signal and noise are taken into account by direct numerical solution of the stochastic generalized nonlinear Schrödinger equation (GNSE) describing transmission in fibers. The limitations we impose on capacity evaluation, notably on the constellation, on memoryless capacity evaluation, and on the dispersion map lead us to refer to our calculated capacity as a conservative estimate (in the spirit of a lower bound) for fiber capacity.

For the most part, Shannon theory [1] has been developed for linear channels that conserve the signal spectral support, i.e., the range of spectral components in a signal. In contrast, a nonlinear channel can, in general, create new frequencies falling outside the spectral support of the input signal, which makes the application of Shannon's theory difficult. A notable exception is a soliton [14], which is a solution of the nonlinear Schrödinger equation (NSE) [15,16] that preserves its spectrum upon nonlinear transmission. However, solitons represent isolated single-symbol solutions of the (noiseless) NSE while capacity calculations need to address sending sequences of symbols both in time and in frequency. We do not consider solitons in this study, but they represent an interesting concept to explore further.

Our approach to deal with the difficulties associated with fiber nonlinearity is to place ourselves in a regime of operation where we believe Shannon's approach should approximately hold. Such a regime limits spectral broadening by fulfilling the condition $L_B \gg L$, where L_B is the transmission length over which a non-negligible amount of spectral components are generated beyond the signal spectral support and L is the transmission path length. To keep L_B large, we operate in the regime $L_D \ll L_{\mathrm{NL}}$, where L_D is the dispersion length and L_{NL} is the nonlinear length [16]. The latter regime is often referred to as pseudolinear transmission [17].

There are two important sources of noise resulting from transmission over optical fibers: double Rayleigh backscattering (DRB) [18] and amplified spontaneous emission (ASE). Since for DRB the backscattered light propagates over a significant fiber length in the backward direction before being scattered back in the forward direction, optical isolators can be inserted along the line to suppress the backward propagation of DRB. Note that the insertion of isolators makes the fiber unidirectional for signal transmission. From the expressions of single Rayleigh backscattering [18], one can easily show that, for distributed amplification with gain compensating fiber loss, the ratio of DRB power to signal power is $\propto 1/N$, where N is the number of (lossless) optical isolators in the line. For sufficiently large values of N, DRB is suppressed. Therefore, DRB does not appear to be as fundamental as ASE as a source of noise and will not be considered further.

The evolution of the optical field $E(z, t)$ in a fiber using distributed Raman amplification with ASE generation can be represented by the stochastic GNSE [19],

$$\frac{\partial E}{\partial z} + \frac{i}{2}\beta_2 \frac{\partial^2 E}{\partial t^2} - i\gamma|E|^2 E = i\mathbf{n}(z, t), \quad (1)$$

where β_2 describes the fiber chromatic dispersion, hereafter simply referred to as dispersion, which is responsible for introducing memory in the channel. Note that the variation of dispersion with frequency is neglected since it is a second-order effect relative to the dispersion itself (except for near-zero values of dispersion) and because fiber can be engineered to have constant dispersion with frequency [20]. To first-order in fiber nonlinearity, the memory, in units of symbols, associated with nonlinear propagation is $\sim(\beta_2 L)_{\max}\Delta f/S$ where $(\beta_2 L)_{\max}$ is the maximum excursion of cumulative signal dispersion in the line, Δf is the input signal bandwidth, and S is the symbol rate. The parameter γ in Eq. (1) is the instantaneous Kerr nonlinearity coefficient [16]. Ideal optical dispersion compensation (lossless and linear) and ideal optical filtering are periodically applied to the signal every L_A km. We use reverse propagation (''back propagation'') by setting the right-hand side of Eq. (1) to zero and changing z to $-z$. All signal-signal nonlinear interactions occurring within one WDM channel are undone by this process. Note that the periodic insertion of perfectly rectangular optical filters is not included in the reverse propagation since this filtering operation cannot be easily inverted.

The term $\mathbf{n}(z, t)$ in Eq. (1) is the term describing ASE noise generation. In Refs. [21,22], Gordon demonstrated that ASE can be represented by a classical field that has the statistical properties of additive Gaussian noise. The establishment of this equivalent representation allows modeling ASE as circularly symmetric complex Gaussian noise, fully characterized by its autocorrelation [23]

$$\langle \mathbf{n}(z, t)\mathbf{n}^*(z', t')\rangle = n_{\mathrm{sp}} K_T h\nu_s \alpha \delta(z - z', t - t'), \quad (2)$$

where n_{sp} is the spontaneous emission factor, ν_s the optical frequency of the signal, α the fiber loss coefficient, and δ is the Dirac functional. The parameter $K_T = 1 + \eta(T)$ is the phonon occupancy factor, where $\eta(T) = 1/\{\exp[h(\nu_p - \nu_s)/(k_B T)] - 1\}$ [24] with k_B the Boltzmann constant, T the fiber temperature, and ν_p the optical frequency of the Raman pump providing the distributed gain. The factor K_T is close to 1 (typically between 1.1 and 1.2) for Raman amplification of fiber-optic communication systems.

We choose an ideal distributed amplification scheme, in which the Raman gain exactly compensates for the fiber intrinsic loss. This choice is motivated by first considering that the delivered optical SNR (OSNR) for a signal of input power P_s over a transmission length L (N spans of length L_A) is given by $2\exp(-\alpha' L_A)P_s/(Nh\nu B_{\mathrm{ref}} F)$ where α' is the net loss (distributed gain minus intrinsic loss) coefficient, $h\nu$ is the photon energy, B_{ref} a reference bandwidth of 12.5 GHz, and F is the noise figure of distributed amplification. The nonlinear phase is given by $\Phi_{\mathrm{NL}}(L) = N\int_0^{L_A} \gamma P_s(z)dz$ [16]. One can show [25] that the maximum value of OSNR at constant Φ_{NL} (and F) occurs when $\alpha' = 0$, i.e., when the distributed gain exactly compensates fiber loss. Experimental demonstrations of nearly ideal distributed gain can be found in Refs. [26,27]. In systems where Raman gain continuously compensates fiber loss, the spectral density N_{ASE} of the noise per polarization at a frequency ν is given by $h\nu K_T \alpha L$. The OSNR at the end of such a line is given by $\mathrm{OSNR} = P_s/(2N_{\mathrm{ASE}}B_{\mathrm{ref}})$ where P_s is the signal power of the WDM channel of interest. For signals using a single state of polarization, the SNR and OSNR are simply related by $\mathrm{SNR} = (2B_{\mathrm{ref}}/S)\,\mathrm{OSNR}$. We assume that the parameters β_2, γ, n_{sp}, ν_s, ν_p, and α are known at both the transmitter and receiver.

We treat the channel as a memoryless channel [1,28,29], in part motivated by the removal of the memory associated with signal-signal intrachannel nonlinearities from the implemented noiseless and filterless reverse propagation. Two additional reasons for using a memoryless channel are that we are thereby lower-bounding the capacity of the channel with memory, and that computations simplify. More precisely, one can show that the channel capacity with memory is lower-bounded by the capacity C for a memoryless channel with input-output conditional probability $p_{Y|X}(y|x)$ and input distribution $p_X(x)$, which is given by

$$C/B = \iint p_{X,Y}(x, y)\log_2 \frac{p_{Y|X}(y|x)}{\int p_{X,Y}(z, y)dz}\, dydx, \quad (3)$$

where B is the bandwidth of the frequency band assigned to each WDM channel and $p_{X,Y}(x, y) = p_X(x)p_{Y|X}(y|x)$. It is well known from Shannon's work that the optimum probability density (PDF) $p_X(x)$ of a band-limited channel with AWGN and input constrained to power P_s is Gaussian distributed of the form [1,28,29],

$$p_X(x) = \frac{1}{\pi P_s} e^{-(x_R^2 + x_I^2)/P_s}, \quad (4)$$

where x_R and x_I are the real and imaginary parts (or cosine and sine components) of the input x. The suboptimal alphabet that we use approximates Eq. (4) by using an alphabet based on concentric rings. We choose the rings equally spaced in optical field amplitude and with equal frequencies of occupation for each ring. The ring amplitudes and occupation frequencies could both still be optimized to better approximate Eq. (4) but, as we shall see later, our constellation choice already gives capacities very close to the Shannon limit for the AWGN channel. We constrain ourselves to this choice of constellation for the nonlinear capacity estimation.

The capacity evaluation can be performed by considering only the angle of rotation relative to its input modulation angle for each constellation point. This is equivalent to backrotating each constellation point by its input modula-

tion angle. The noisy and nonlinearly distorted clouds are fitted for each ring to bivariate Gaussian PDFs whose covariance matrices capture cloud noncircularity. From these PDFs and Eq. (3), one can calculate capacity estimates. We also explored fitting non-Gaussian PDF shapes, both with and without circular symmetry. These PDFs led to very marginally different capacities than obtained for the bivariate Gaussian PDFs.

Each symbol modulates a near Nyquist ("sinc") pulse in the time domain [13], which limits the signal support to a bandwidth equal to the symbol rate S. This is shown in Fig. 1(a) which gives an example of a signal on a 2-ring constellation shown in Fig. 1(b) with 32 symbols. The corresponding field amplitude waveform is shown in Fig. 1(c).

The capacity of the constrained ring constellations in the absence of fiber nonlinearity is shown by the set of curves enclosed by the ellipse on the upper part of Fig. 2. Shannon's limit, given by $C/S = \log_2(1 + \mathrm{SNR})$ bits/symbol, is also shown as a reference. The symbol rate S is 100 Gbaud and the channel bandwidth B is 102 GHz, the latter incorporating the 2-GHz guard band. Optical routing is performed by placing rectangular optical filters of 102-GHz bandwidth at the end of each span. We have also studied bandwidths of 100 and 101 GHz and obtained virtually identical results. Rectangular filters are used because they approximately match the signal spectrum even after propagation and because they are infinitely cascadable. At a given SNR in the range of interest, there is a sufficient number of rings that allows us to very closely approach the Shannon limit. For this number of rings, the uniformly spaced ring constellation with uniform occupancy is virtually optimal. We now calculate a fiber capacity estimate for optically routed networks. We consider a link of 2000 km (20 spans of 100 km) of standard single-mode fiber having $\beta_2 = -21.67\ \mathrm{ps^2\,km^{-1}}$, $\gamma = 1.27\ (\mathrm{W\,km})^{-1}$, and a loss of 0.2 dB/km. The wavelengths of the signal and Raman pump, λ_s and λ_p, are set to 1550 and 1450 nm, respectively. Constellations with 1, 2, 4, 8, and 16 rings are shown. A dispersion map with optimum precompensation [30] and optimum residual dispersion per span for transmission in the absence of nonlinearity compensation at the transmitter or receiver is used. The cumulative dispersion is brought back to zero before entering the coherent receiver. We modeled transmission with a large number of WDM channels and found that five WDM channels were sufficient to capture all WDM nonlinear effects. The 2048 constellation points are randomly chosen on the ring constellation structure. The large computation time prevented the use of larger numbers of points but repeated trials with different noise and data realizations led to variations in capacity estimates of a few tenths of bits/s/Hz. Reverse propagation applied at both the transmitter and receiver in variable ratios also produced capacity estimates within an accuracy estimated to be a few tenths of bits/s/Hz.

The fiber channel capacity per unit bandwidth for the nonlinear system studied is displayed by the curves with symbols in Fig. 2. For each number of rings, the capacity increases following the linear capacity curves at low SNR, until it saturates around an SNR of ~20 dB. This saturation is caused by nonlinear distortions originating mainly from interchannel fiber nonlinearities that increase the clouds' sizes associated to each ring as seen in Fig. 3. Further power increase results in a decrease in capacity. For our system, $L_D \equiv (S^2|\beta_2|)^{-1} = 4.61$ km and, for a SNR of 20 dB, $L_{\mathrm{NL}} = (\gamma P_{\mathrm{ave}})^{-1} = 5890$ km that corresponds to $L_{\mathrm{NL}} \sim 1000 L_D$ so that we are well within the pseudolinear transmission regime. The signal does not

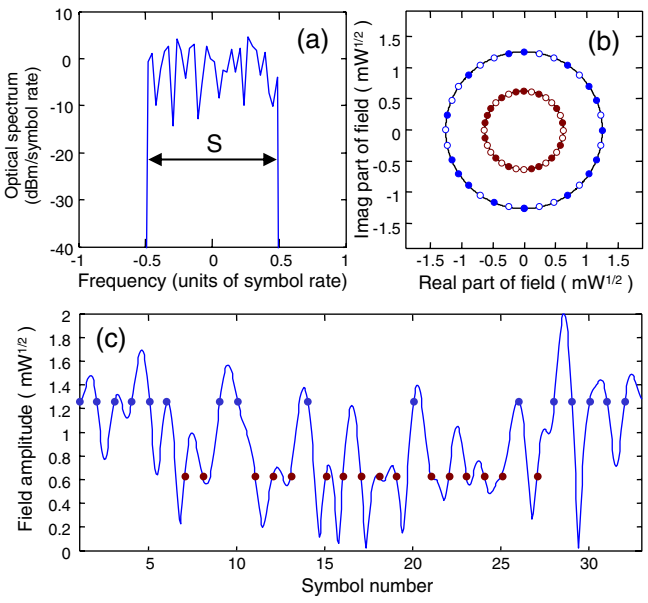

FIG. 1 (color online). Example of a modulated optical field used in this study: (a) Spectrum; (b) symbol realization and constellation; and (c) sampling instants of the corresponding analog waveform. The average power is 1 mW.

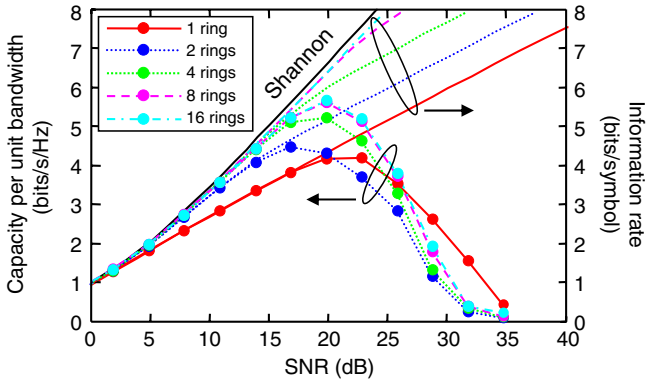

FIG. 2 (color online). Information rate and fiber channel capacity for ring constellations. Right axis: information rate in the absence of fiber nonlinearity; Left axis: fiber capacity when taking into account fiber nonlinearity for a 2000-km system described in the text. A maximum of ~5.6 bits/s/Hz per polarization state is obtained for 16 rings.

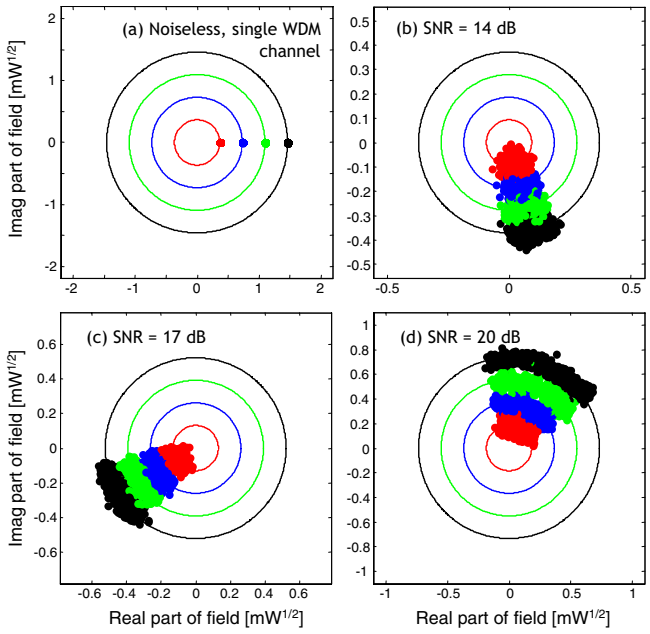

FIG. 3 (color online). Backrotated constellations after transmission: (a) without ASE (noise) and fiber nonlinearity. Graphs (b), (c), and (d) are with noise and fiber nonlinearity for different SNR. Note that nonlinear distortions tend to spread the constellation points along the modulation circle they belong to.

broaden significantly to interfere with neighboring WDM channels despite the tight channel packing. The maximum capacity increases with the number of rings and reaches ~5.6 bits/s/Hz for 16 rings. The multiple-ring and one-ring curves cross at high SNR (beyond SNRs of highest capacities) in Fig. 2 because we have not optimized the ring occupation frequencies and ring amplitudes. The maximum spectral efficiency in Fig. 2 exceeds by a factor ~3 in spectral efficiency per polarization the current high-capacity record experiment [31] established over a much shorter distance, suggesting that advanced technologies can be highly beneficial to increase fiber capacity.

This project was supported by DARPA under Contract No. HR0011-06-C-0098. We gratefully acknowledge discussions with Robert W. Tkach, James P. Gordon, Andrew R. Chraplyvy, Adel A. M. Saleh, Alan Gnauck, Aref Chowdhury, Herwig Kogelnik, and hardware modeling support from Ellsworth C. Burrows.

*rjessiam@alcatel-lucent.com

[1] C. E. Shannon, Bell Syst. Tech. J. **27**, 379 (1948); **27**, 623 (1948).
[2] E. Desurvire, Opt. Fiber Technol. **8**, 210 (2002).
[3] J. Tang, J. Lightwave Technol. **19**, 1104 (2001).
[4] P. P. Mitra and J. B. Stark, Nature (London) **411**, 1027 (2001).
[5] E. Narimanov and P. P. Mitra, J. Lightwave Technol. **20**, 530 (2002).
[6] J. Tang, J. Lightwave Technol. **20**, 1095 (2002).
[7] K. S. Turitsyn, S. A. Derevyanko, I. V. Yurkevich, and S. K. Turitsyn, Phys. Rev. Lett. **91**, 203901 (2003).
[8] L. G. L. Wegener, M. L. Povinelli, A. G. Green, P. P. Mitra, J. B. Stark, and P. B. Littlewood, Physica (Amsterdam) **189D**, 81 (2004).
[9] M. H. Taghavi, G. C. Papen, and P. H. Siegel, IEEE Trans. Inf. Theory **52**, 5008 (2006).
[10] K.-P. Ho, in Proceedings of the Optical Fiber Communications Conference (OFC) (Optical Society of America, Anaheim, 2002), p. 731, PAPER ThGG85.
[11] I. Djordjevic, B. Vasic, M. Ivkovic, and I. Gabitov, J. Lightwave Technol. **23**, 3755 (2005).
[12] R.-J. Essiambre, G. J. Foschini, P. J. Winzer, G. Kramer, and E. C. Burrows, in Proceedings of the Optical Fiber Communications Conference (OFC) (Optical Society of America, San Diego, 2008), OTuE1.
[13] H. Nyquist, Trans. Am. Inst. Electr. Eng. **47**, 617 (1928).
[14] L. F. Mollenauer, R. H. Stolen, and J. P. Gordon, Phys. Rev. Lett. **45**, 1095 (1980).
[15] A. Hasegawa and F. Tappert, Appl. Phys. Lett. **23**, 142 (1973).
[16] G. P. Agrawal, *Nonlinear Fiber Optics* (Elsevier Science & Technology, San Diego, 2006), 4th ed.
[17] R.-J. Essiambre, G. Raybon, and B. Mikkelsen, in *Optical Fiber Telecommunications IV*, edited by I. Kaminow and T. Li (Academic Press, San Diego, 2002), pp. 232–304.
[18] J. Bromage, P. J. Winzer, and R.-J. Essiambre, in *Raman Amplifiers and Oscillators in Telecommunications*, edited by M. N. Islam (Springer Verlag, Berlin, 2003).
[19] C. W. Gardiner, *Handbook of Stochastic Methods: for Physics, Chemistry and the Natural Science* (Springer, New York, 2004), 3rd ed.
[20] R. Lundin, Appl. Opt. **33**, 1011 (1994).
[21] J. P. Gordon, W. H. Louisell, and L. R. Walker, Phys. Rev. **129**, 481 (1963).
[22] J. P. Gordon, L. R. Walker, and W. H. Louisell, Phys. Rev. **130**, 806 (1963).
[23] A. Mecozzi, J. Lightwave Technol. **12**, 1993 (1994).
[24] J. Bromage, J. Lightwave Technol. **22**, 79 (2004).
[25] V. E. Perlin and H. G. Winful, IEEE Photonics Technol. Lett. **14**, 1199 (2002).
[26] J.-C. Bouteiller, K. Brar, J. Bromage, S. Radic, and C. Headley, IEEE Photonics Technol. Lett. **15**, 212 (2003).
[27] T. J. Ellingham, J. D. Ania-Castañon, R. Ibbotson, X. Chen, L. Zhang, and S. K. Turitsyn, IEEE Photonics Technol. Lett. **18**, 268 (2006).
[28] R. G. Gallager, *Information Theory and Reliable Communication* (John Wiley and Sons, New York, 1968), Chaps. 2 and 4.
[29] T. M. Cover and J. A. Thomas, *Elements of Information Theory* (John Wiley and Sons, New York, 1991), Chaps. 2 and 8.
[30] A. Mecozzi, C. B. Clausen, M. Shtaif, S.-G. Park, and A. H. Gnauck, IEEE Photonics Technol. Lett. **13**, 445 (2001).
[31] A. H. Gnauck, G. Charlet, P. Tran, P. J. Winzer, C. R. Doerr, J. Centanni, E. C. Burrows, T. Kawanishi, T. Sakamoto, and K. Higuma, Proceedings of the Optical Fiber Communications Conference (OFC) (Optical Society of America, Anaheim, 2007), PDP19.